

NASA/TP-2009-215941



# Coupled Neutron Transport for HZETRN

*Tony C. Slaba*  
*Old Dominion University, Norfolk, Virginia*

*Steve R. Blattig*  
*Langley Research Center, Hampton, Virginia*

---

October 2009

## NASA STI Program . . . in Profile

Since its founding, NASA has been dedicated to the advancement of aeronautics and space science. The NASA scientific and technical information (STI) program plays a key part in helping NASA maintain this important role.

The NASA STI program operates under the auspices of the Agency Chief Information Officer. It collects, organizes, provides for archiving, and disseminates NASA's STI. The NASA STI program provides access to the NASA Aeronautics and Space Database and its public interface, the NASA Technical Report Server, thus providing one of the largest collections of aeronautical and space science STI in the world. Results are published in both non-NASA channels and by NASA in the NASA STI Report Series, which includes the following report types:

- **TECHNICAL PUBLICATION.** Reports of completed research or a major significant phase of research that present the results of NASA programs and include extensive data or theoretical analysis. Includes compilations of significant scientific and technical data and information deemed to be of continuing reference value. NASA counterpart of peer-reviewed formal professional papers, but having less stringent limitations on manuscript length and extent of graphic presentations.
- **TECHNICAL MEMORANDUM.** Scientific and technical findings that are preliminary or of specialized interest, e.g., quick release reports, working papers, and bibliographies that contain minimal annotation. Does not contain extensive analysis.
- **CONTRACTOR REPORT.** Scientific and technical findings by NASA-sponsored contractors and grantees.

- **CONFERENCE PUBLICATION.** Collected papers from scientific and technical conferences, symposia, seminars, or other meetings sponsored or co-sponsored by NASA.
- **SPECIAL PUBLICATION.** Scientific, technical, or historical information from NASA programs, projects, and missions, often concerned with subjects having substantial public interest.
- **TECHNICAL TRANSLATION.** English-language translations of foreign scientific and technical material pertinent to NASA's mission.

Specialized services also include creating custom thesauri, building customized databases, and organizing and publishing research results.

For more information about the NASA STI program, see the following:

- Access the NASA STI program home page at <http://www.sti.nasa.gov>
- E-mail your question via the Internet to [help@sti.nasa.gov](mailto:help@sti.nasa.gov)
- Fax your question to the NASA STI Help Desk at 443-757-5803
- Phone the NASA STI Help Desk at 443-757-5802
- Write to:  
NASA STI Help Desk  
NASA Center for AeroSpace Information  
7115 Standard Drive  
Hanover, MD 21076-1320

NASA/TP-2009-215941



# Coupled Neutron Transport for HZETRN

*Tony C. Slaba*  
*Old Dominion University, Norfolk, Virginia*

*Steve R. Blattmig*  
*Langley Research Center, Hampton, Virginia*

National Aeronautics and  
Space Administration

Langley Research Center  
Hampton, Virginia 23681-2199

October 2009

Available from:

NASA Center for AeroSpace Information  
7115 Standard Drive  
Hanover, MD 21076-1320  
443-757-5802

## Abbreviations

DC	Directionally Coupled neutron transport model
FB	Forward Backward neutron transport model
FLUKA	FLUctuating KAskade
GCR	Galactic Cosmic Rays
HETC-HEDS	High Energy Transport Code – Human Exploration and Development of Space
HZETRN	High charge (Z) and Energy TRANsport code
LEO	Low Earth Orbit
LU	Lower-Upper
MCNPX	Monte Carlo Neutral Particle eXtended
SA	Straight Ahead
SPE	Solar Particle Event

## Contents

Abstract .....	1
1. Introduction .....	1
2. HZETRN Description .....	2
3. Neutron Transport Models .....	4
4. FB Neutron Transport Methods .....	11
5. DC Neutron Transport Methods .....	13
6. Coupling to Light Ion Transport .....	14
7. Results .....	15
8. Conclusions .....	19
9. Acknowledgments .....	20
10. References .....	20

## Figures

1.	Forward (+), backward (-), and total neutron nuclear reactive production cross section for a 500 MeV proton projectile and Aluminum target.....	6
2.	Straight ahead (sa), isotropic (iso), and total neutron nuclear reactive production cross section for a 500 MeV proton projectile and Aluminum target.....	7
3.	Neutron and $^4\text{He}$ fluence spectra at $50 \text{ g/cm}^2$ in an Aluminum target exposed to the February, 1956 Webber SPE.....	7
4.	Range and mean free path length of $^4\text{He}$ in Aluminum. ....	9
5.	Forward neutron fluence at $20 \text{ g/cm}^2$ in a $30 \text{ g/cm}^2$ water target behind a $20 \text{ g/cm}^2$ Aluminum shield exposed to the February, 1956 Webber SPE.....	16
6.	Backward neutron fluence at $20 \text{ g/cm}^2$ in a $30 \text{ g/cm}^2$ water target behind a $20 \text{ g/cm}^2$ Aluminum shield exposed to the February, 1956 Webber SPE. ....	16
7.	Total neutron fluence at $20 \text{ g/cm}^2$ in a $30 \text{ g/cm}^2$ water target behind a $20 \text{ g/cm}^2$ Aluminum shield exposed to the February, 1956 Webber SPE.....	17
8.	Proton fluence at $20 \text{ g/cm}^2$ in a $30 \text{ g/cm}^2$ water target behind a $20 \text{ g/cm}^2$ Aluminum shield exposed to the February, 1956 Webber SPE.....	17
9.	$^3\text{H}$ fluence at $20 \text{ g/cm}^2$ in a $30 \text{ g/cm}^2$ water target behind a $20 \text{ g/cm}^2$ Aluminum shield exposed to the February, 1956 Webber SPE.....	18
10.	$^4\text{He}$ fluence at $20 \text{ g/cm}^2$ in a $30 \text{ g/cm}^2$ water target behind a $20 \text{ g/cm}^2$ Aluminum shield exposed to the February, 1956 Webber SPE.....	18

## Tables

1. Dose (cGy) in a  $30 \text{ g/cm}^2$  water target behind  $20 \text{ g/cm}^2$  of Aluminum exposed to the February, 1956 Webber SPE spectrum. ....19
2. Dose equivalent (cSv) in a  $30 \text{ g/cm}^2$  water target behind  $20 \text{ g/cm}^2$  of Aluminum exposed to the February, 1956 Webber SPE spectrum. ....19

## Abstract

*Exposure estimates inside space vehicles, surface habitats, and high altitude aircraft exposed to space radiation are highly influenced by secondary neutron production. The deterministic transport code HZETRN (High charge (Z) and Energy TRAnsport) has been identified as a reliable and efficient tool for such studies, but improvements to the underlying transport models and numerical methods are still necessary. In this paper, the forward-backward (FB) and directionally coupled forward-backward (DC) neutron transport models are derived, numerical methods for the FB model are reviewed, and a computationally efficient numerical solution is presented for the DC model. Both models are compared to the Monte Carlo codes HETC-HEDS (High Energy Transport Code – Human Exploration and Development of Space), FLUKA (FLUctuating KAskade), and MCNPX (Monte Carlo Neutral Particle eXtended), and the DC model is shown to agree closely with the Monte Carlo results. Finally, it is found in the development of either model that the decoupling of low energy neutrons from the light particle transport procedure adversely affects low energy light ion fluence spectra and the subsequent exposure quantities. A first order correction is presented to resolve the problem, and it is shown to be both accurate and efficient.*

## 1. Introduction

Radiation exposure guidelines are a primary concern for the design of personal shielding, spacecraft, instrumentation, and missions. Consequently, there is significant interest in developing computational tools that allow shield analyses not only in simplified geometries, but in more complex final design models as well [Wilson et al. 2003]. The deterministic transport code HZETRN [Wilson et al. 1991, 2006; Slaba et al. 2008], developed at NASA Langley Research Center has emerged in recent years as a reliable and efficient tool for such studies. It has shown reasonable accuracy in deep space Galactic Cosmic Ray (GCR), Solar Particle Event (SPE), and Low Earth Orbit (LEO) simulations when compared to either Monte Carlo results or experimental data [Wilson et al. 2005; Heinbockel et al. 2009]. However, such verification and validation has revealed a deficiency in the low energy neutron transport procedure [Shinn et al. 1994; Heinbockel et al. 2009]. HZETRN utilizes the straight ahead approximation in which all fragments are assumed to propagate in the same direction as the projectile. The assumption is accurate for high energy charged particles but begins to break down for low energy neutrons which are nearly isotropic [Alsmiller et al. 1965]. This is significant for heavily shielded space vehicles, surface habitats, and high altitude aircraft where secondary neutron production is important in exposure calculations [Getselev et al. 2004].

Several neutron transport models have been developed for HZETRN, with recent efforts focused on identifying an optimal bi-directional neutron transport model and solution method. The terms model and method are used extensively throughout this paper; model is used to refer to the set of governing transport equations, while method is used to refer to the analytic or numerical techniques used to solve a model. Heinbockel et al. [2000] and Cloudsley et al. [2000a, 2000b] developed the forward-backward (FB) neutron transport model. The FB model assumes that low energy neutrons can be split into forward and backward components, and multiple reflections from forward to backward (or vice versa) can be ignored. Feldman [2003] expanded on the work of Heinbockel and Cloudsley by developing the directionally coupled forward-backward (DC) neutron transport model. The DC model also assumes that low energy neutrons can be split into forward and backward components, but multiple reflections are accounted for in the governing transport equations. The numerical methods used for each model were significantly different as well.

Heinbockel et al. [2000] and Cloudsley et al. [2000a, 2000b] used a multigroup method for solving the FB model. Multigroup methods have a long history in nuclear reactor theory and assume that fluences or cross sections are constant over small regions, or groups, of the energy spectrum [Marchuk and Lebedev 1986]. Feldman [2003] used a collocation technique along with first order finite differencing for the DC model. Collocation and finite differencing methods use polynomial expansions of the solution to

transform a differential equation into a system of linear equations [Deuflhard and Bornemann 2002]. In this case, the system was sufficiently large that it had to be solved numerically.

Recently, Slaba et al. [2006, 2007] and Heinbockel et al. [2007] developed three methods for solving the FB model which they called the collocation method, the fixed-point series method, and Wilson's method. The latter two methods are both based on a Neumann series solution wherein each term of the series solves a simple set of equations related to the original model. This allowed for intensive verification of the multigroup method, and the collocation method was identified as the most accurate and computationally efficient of all the methods [Slaba 2007]. Slaba [2007] also indicated that a combination of the methods could be used to obtain a computationally efficient Neumann series solution to the DC model. Finally, despite all of the attention given to neutron transport models and methods, accurately coupling these models back into HZETRN remained unresolved. The impact of such a coupling has not been previously studied in detail and must be examined if any of the neutron transport models are to be used in design studies.

In this paper, we first give a summary of the neutron transport models and methods developed thus far and present an efficient method for solving the DC model. Next, comparisons are made between the FB and DC models and the Monte Carlo codes HETC-HEDS [Gabriel et al. 1995; Townsend et al. 2005], FLUKA [Fasso et al. 2003, 2005], and MCNPX [Briesmeister, 2000; MCNPX 2.6.0 Manual, 2008]. Finally, the impact of decoupling low energy neutrons from the light ion transport procedure in HZETRN is also examined, and a first order coupling is presented. Fluence spectra and dose quantities are given to exhibit the accuracy of the proposed correction.

## 2. HZETRN Description

The one-dimensional Boltzmann transport equation for charged and neutral particles with the continuous slowing down and straight ahead approximations is given as [Wilson et al. 1991]

$$B[\phi_j] = \sum_k \int_E^\infty \sigma_{jk}(E, E') \phi_k(x, E') dE', \quad (1)$$

with the linear differential operator

$$B[\phi_j] \equiv \left[ \frac{\partial}{\partial x} - \frac{1}{A_j} \frac{\partial}{\partial E} S_j(E) + \sigma_j(E) \right] \phi_j, \quad (2)$$

where  $\phi_j$  is the fluence of type  $j$  ions at depth  $x$  with kinetic energy  $E$  (MeV/amu),  $A_j$  is the atomic mass of a type  $j$  particle,  $S_j(E)$  is the stopping power of a type  $j$  ion with kinetic energy  $E$ ,  $\sigma_j(E)$  is the total macroscopic cross section for a type  $j$  particle with kinetic energy  $E$ , and  $\sigma_{jk}(E, E')$  is the macroscopic production cross section for interactions in which a type  $k$  particle with kinetic energy  $E'$  produce a type  $j$  particle with kinetic energy  $E$ . Macroscopic cross sections are obtained by multiplying the corresponding microscopic cross section by the target particle mass density [Wilson et al. 1991]. Hereafter, it is assumed that all cross sections are macroscopic whether it is explicitly written or not. The summation over  $k$  on the right hand side of equation (1) will be explained shortly.

Wilson et al. [1986, 1991, 2006] obtained approximate solutions to equation (1) by introducing the scaled quantities

$$\psi_j(x, r) \equiv \nu_j S_p(E) \phi_j(x, E), \quad (3)$$

$$s_{jk}(r, r') \equiv S_p(E) \sigma_{jk}(E, E'), \quad (4)$$

where  $S_p(E)$  is the proton stopping power,  $r$  is the residual proton range

$$r \equiv \int_0^E \frac{dE'}{S_p(E')}, \quad (5)$$

the scaling parameter  $\nu_j \equiv Z_j^2 / A_j$ , and  $Z_j$  is the charge of a type  $j$  ion. For neutrons,  $\nu$  is taken as unity in fluence scaling relations and zero in range scaling relations. This will be explained in more detail shortly. Equation (1) is now given in terms of the variables  $x$  and  $r$  as

$$\left[ \frac{\partial}{\partial x} - \nu_j \frac{\partial}{\partial r} + \sigma_j(r) \right] \psi_j(x, r) = \sum_k \frac{\nu_j}{\nu_k} \int_r^\infty s_{jk}(r, r') \psi_k(x, r') dr', \quad (6)$$

which can be inverted using the method of characteristics [Haberman 1998] and written as the Volterra type integral equation [Wilson et al. 2006]

$$\begin{aligned} \psi_j(x, r) = & e^{-\varsigma_j(r, x)} \psi_j(0, r + \nu_j x) \\ & + \sum_k \frac{\nu_j}{\nu_k} \int_0^x \int_{r + \nu_j x'}^\infty e^{-\varsigma_j(r, x')} s_{jk}(r + \nu_j x', r') \psi_k(x - x', r') dr' dx', \end{aligned} \quad (7)$$

with the exponential attenuation term

$$\varsigma_j(r, x) \equiv \int_0^x \sigma_j(r + \nu_j t) dt. \quad (8)$$

Note that  $\nu_j$  in equation (3) and  $\nu_j / \nu_k$  in equation (6) are both fluence scaling relations, and  $\nu_n = 1$  in both cases to provide a nontrivial scaling. Conversely, wherever  $\nu$  appears as the argument of a fluence or cross section in equations (7) and (8), it is a range scaling relation and  $\nu_n = 0$ . This convention is taken to reflect the absence of atomic interactions in neutron transport ( $S_n(E) \equiv 0$ ) and to avoid a trivial scaling for the neutron fluence.

From here, the problem is split into two parts: heavy ions ( $A > 4$ ) and light particles ( $A \leq 4$ ). For heavy ions, it is noted that projectile fragments have energy and direction very near that of the projectile (equal velocity assumption), while target fragments are produced nearly isotropically with low energy and travel only a short distance before being absorbed. This approximate decoupling of target and projectile fragments is discussed in detail by Wilson et al. [1991] and suggests that target fragments can be neglected in the heavy ion transport procedure (their contribution to dose is approximately accounted for after the transport procedure). The equal velocity assumption allows the production cross section to be recast as

$$s_{jk}(r, r') = \sigma_{jk}(r) \delta(r - r'), \quad (9)$$

or equivalently, in terms of energy as

$$\sigma_{jk}(E, E') = \sigma_{jk}(E) \delta(E - E'). \quad (10)$$

Note that  $\sigma_{jk}(E)$  can be written interchangeably with  $E$  or  $r$  since, for a given  $E$ , equation (5) can be evaluated to obtain  $r$ . The absence of target fragments in the heavy ion transport procedure allows one to take the summation in equation (7) over all projectiles with mass greater than that of the fragment. If all

transported heavy ions are ordered according to mass, then the final marching procedure for heavy ions is given by [Wilson et al. 2006]

$$\begin{aligned} \psi_j(x+h, r) &= e^{-\zeta_j(r, h)} \psi_j(x, r + \nu_j h) \\ &+ \sum_{k>j} \frac{\nu_j}{\nu_k} \sigma_{jk} \left( r + \nu_j \frac{h}{2} \right) \psi_k \left( x, r + (\nu_j + \nu_k) \frac{h}{2} \right) \\ &\times \left[ \frac{e^{-\sigma_j \left( r + \nu_j \frac{h}{2} \right) h} - e^{-\sigma_k \left( r + (\nu_j + \nu_k) \frac{h}{2} \right) h}}{\left[ \sigma_k \left( r + (\nu_j + \nu_k) \frac{h}{2} \right) - \sigma_j \left( r + \nu_j \frac{h}{2} \right) \right]} \right] \\ &+ O(h^2), \end{aligned} \quad (11)$$

where  $h$  is the step size in  $\text{g/cm}^2$ . The summation over all  $k > j$  reflects the fact that only heavy ion projectiles fragments are explicitly transported and that the transported heavy ions have been ordered according to mass. The upper summation limit in equation (11) can vary, but it is now common to use no fewer than 59 isotopes. See Cucinotta et al. [2006] for a discussion of isotopes grids.

For light particles, both projectile and target fragments are included in the transport procedure; therefore, the summation is taken over all light particles. The broad energy distribution in collision events also indicates that equal velocity assumption cannot be used. The final marching procedure for light particles is given by [Wilson et al. 1991, 2006]

$$\begin{aligned} \psi_j(x+h, r) &= e^{-\zeta_j(r, h)} \psi_j(x, r + \nu_j h) \\ &+ \sum_k \frac{\nu_j}{\nu_k} \int_{r+\nu_j h/2}^{\infty} e^{-\zeta_j \left( r, \frac{h}{2} \right) - \zeta_k \left( r', \frac{h}{2} \right)} F_{jk}^{\Delta}(r, r'; h) \psi_k \left( x, r' + \nu_k \frac{h}{2} \right) dr' \\ &+ O(h^2), \end{aligned} \quad (12)$$

where the integrand has been simplified using

$$F_{jk}^{\Delta}(r, r'; h) \equiv \int_0^h s_{jk}(r + \nu_j z, r') dz, \quad (13)$$

and the neutron elastic interactions in this equation are handled separately as [Slaba et al. 2008]

$$F_{nn}^{\Delta, el}(r, r'; h) \equiv h \left\langle s_{nn}^{el}(r, \Delta r') \right\rangle, \quad (14)$$

where  $F_{nn}^{\Delta, el}(r, r'; h)$  denotes the elastic component and  $\left\langle s_{nn}^{el}(r, \Delta r') \right\rangle$  is the average value of the differential neutron elastic cross section over a small interval,  $\Delta r'$ , centered at  $r'$ .

The nature of the boundary condition, or environment, determines how equations (11) and (12) are evaluated and coupled. For most SPE environments, there is usually a negligible heavy ion component, and only equation (12) is evaluated. For GCR environments, equation (11) is evaluated for heavy ions; equation (12) is evaluated for light particles, and the summation term appearing in equation (11) is added. The summation is taken only over heavy ion projectiles, and it physically accounts for light ion production from heavy ion projectiles. The marching equations (11) and (12) will be referred to throughout this paper as the HZETRN marching algorithm, with the proper equations evaluated and coupled for a given environment.

### 3. Neutron Transport Models

To derive the neutron transport models, we first decompose the particle fluence and neutron production cross section into straight ahead and isotropic components. This approximation is justified by

Wilson et al. [1991] who showed that projectile fragments are produced with energy and direction very near that of the projectile, while target fragments are produced nearly isotropically with very low energy. For particle fluences, the decomposition is given as [Wilson et al. 2005]

$$\phi_j(x, E) = \phi_j^{iso}(x, E) + \phi_j^{sa}(x, E). \quad (15)$$

To decompose the neutron production cross section, we first distinguish between the nuclear reactive and elastic parts

$$\sigma_{nk}(E, E') = \sigma_{nk}^r(E, E') + \sigma_{nk}^{el}(E, E'), \quad (16)$$

where  $\sigma_{nk}^{el}(E, E') = 0$  for  $k \neq n$ . The angularly dependent nuclear reactive neutron production cross section can be represented as [Wilson et al. 2005]

$$\hat{\sigma}_{nk}^r(E, E', \mathbf{\Omega}, \mathbf{\Omega}') = g(A_T, E, \theta) \sigma_{nk}^r(E, E'), \quad (17)$$

where  $\mathbf{\Omega}$  and  $\mathbf{\Omega}'$  are unit vectors in the direction of the secondary neutron and projectile particle, respectively. The parameterization for  $g(A_T, E, \theta)$  is given by the piecewise definition [Ranft, 1980]

$$g(A_T, E, \theta) \equiv \begin{cases} Ne^{-\theta^2/\lambda} & , 0 \leq \theta \leq \pi/2 \\ Ne^{-\pi^2/4\lambda} & , \pi/2 < \theta \leq \pi \end{cases} \quad (18)$$

and  $\lambda \equiv (120 + 0.36A_T) / E$ , where  $E$  is the produced neutron kinetic energy in MeV,  $A_T$  is the atomic mass of the target nucleus,  $\theta$  is the production angle with respect to the direction of propagation, and  $N$  is a normalization constant such that

$$2\pi \int_0^\pi g(A_T, E, \theta) d\theta = 1. \quad (19)$$

The parameterization constants, 120 and 0.36 have units MeV and MeV/amu, respectively, so that  $\lambda$  is dimensionless.

The nuclear reactive neutron production cross section can now be decomposed into forward (scattering angle  $\theta \in [0, \pi/2]$ ) and backward (scattering angle  $\theta \in (\pi/2, \pi]$ ) components

$$\begin{aligned} \sigma_{nk}^r(E, E') &= F^{(+)}(A_T, E) \sigma_{nk}^r(E, E') + F^{(-)}(A_T, E) \sigma_{nk}^r(E, E') \\ &\equiv \sigma_{nk}^{r,(+)}(E, E') + \sigma_{nk}^{r,(-)}(E, E'), \end{aligned} \quad (20)$$

where the forward and backward coefficients are

$$F^{(+)}(A_T, E) \equiv \int_0^{\pi/2} g(A_T, E, \theta) d\theta, \quad (21)$$

$$F^{(-)}(A_T, E) \equiv 1 - F^{(+)}(A_T, E). \quad (22)$$

The straight ahead and isotropic coefficients are therefore defined as [Cloudsley et al. 2000b]

$$F^{sa}(A_T, E) \equiv 1 - F^{iso}(A_T, E), \quad (23)$$

$$F^{iso}(A_T, E) \equiv 2F^{(-)}(A_T, E), \quad (24)$$

so that the nuclear reactive neutron production cross section can be expressed in terms of isotropic and straight ahead components

$$\begin{aligned} \sigma_{nk}^r(E, E') &= F^{sa}(A_T, E)\sigma_{nk}^r(E, E') + F^{iso}(A_T, E)\sigma_{nk}^r(E, E') \\ &\equiv \sigma_{nk}^{r,sa}(E, E') + \sigma_{nk}^{r,iso}(E, E'). \end{aligned} \quad (25)$$

The decompositions in equations (20) and (25) are depicted in Figs. 1 and 2 for a 500 MeV proton projectile and an Aluminum target. It should be noted that in Fig. 2 the straight ahead component of the nuclear reactive neutron production cross section is dominant at high fragment energies, while the isotropic component is dominant at low fragment energies as discussed earlier.

Equations (15), (16) and (25) are substituted into equation (1), and the HZETRN marching algorithm is used to solve the straight ahead transport equation

$$B[\phi_j^{sa}] = \sum_k \int_E^\infty \kappa_{jk}^{sa}(E, E') \phi_k^{sa}(x, E') dE', \quad (26)$$

where the summation limits for equation (26) are environment dependent and have been discussed previously, and the production cross section  $\kappa_{jk}(E, E')$  is piecewise defined as

$$\kappa_{jk}^{sa}(E, E') \equiv \begin{cases} \sigma_{nk}^{r,sa}(E, E') + \sigma_{nk}^{el}(E, E') & , j = n \\ \sigma_{jk}(E, E') & , j \neq n \end{cases} . \quad (27)$$

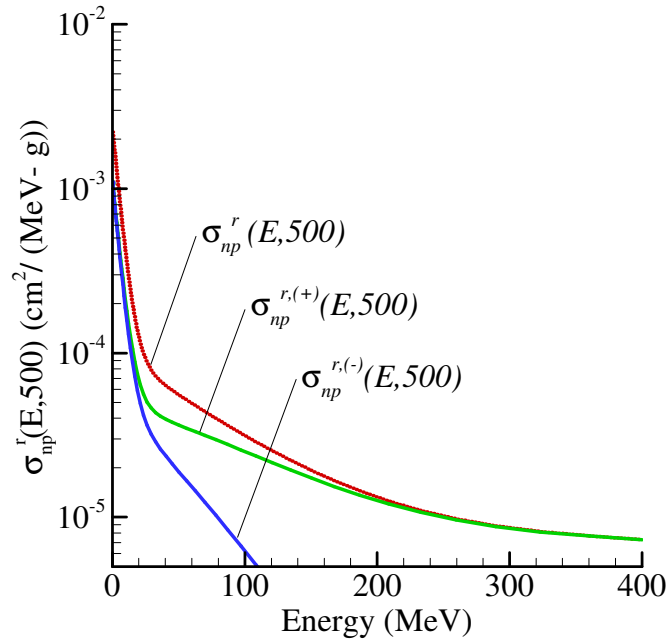


Figure 1. Forward (+), backward (-), and total neutron nuclear reactive production cross section for a 500 MeV proton projectile and Aluminum target.

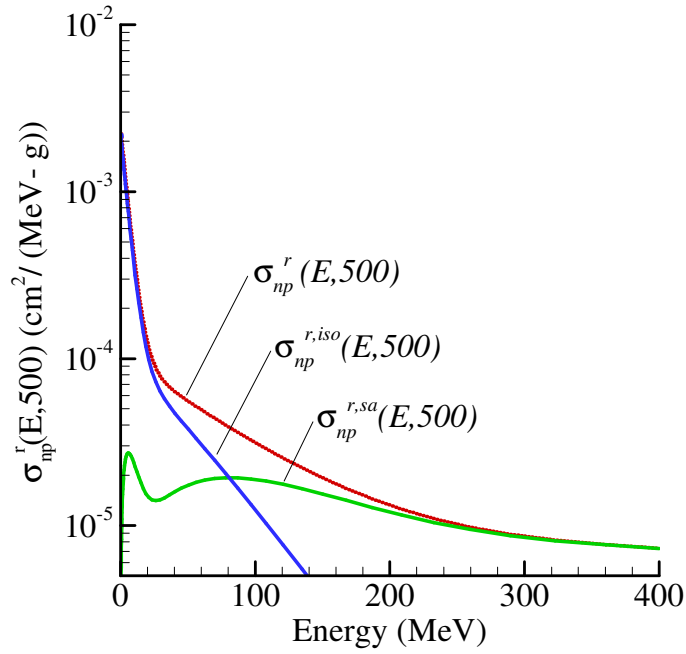


Figure 2. Straight ahead (sa), isotropic (iso), and total neutron nuclear reactive production cross section for a 500 MeV proton projectile and Aluminum target.

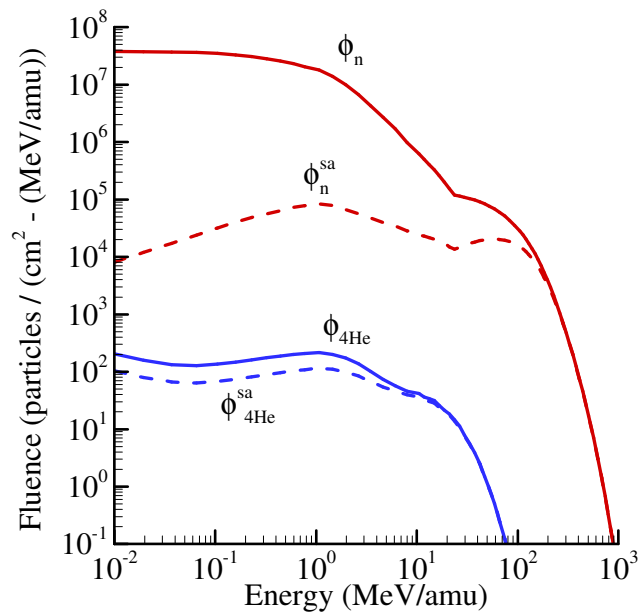


Figure 3. Neutron and  $^4\text{He}$  fluence spectra at  $50 \text{ g/cm}^2$  in an Aluminum target exposed to the February, 1956 Webber SPE.

Note that for light particle projectile/fragment combinations,  $\sigma_{jk}(E, E')$  will be fully energy dependent, while for heavy ion projectiles,  $\sigma_{jk}(E, E')$  incorporates the equal velocity assumption and assumes the simplified form in equation (10).

The only difference between equations (1) and (26) is the form of the neutron production cross section; equation (1) uses the total nuclear reactive neutron production cross section, while equation (26) uses only the straight ahead component. Fig. 2 suggests that neutron fluences obtained from equation (26) will have attenuated low energy spectra, and an examination of the HZETRN marching algorithm indicates that a residual attenuation will occur in the low energy light ion spectra as well. This behavior is evident in Fig. 3. More will be said about this later.

We are now left to solve for the isotropic neutron fluence

$$B[\phi_n^{iso}] = \sum_k \int_E^\infty \sigma_{nk}(E, E') \phi_k^{iso}(x, E') dE' + \eta_n(x, E), \quad (28)$$

with the isotropic neutron source term

$$\eta_n(x, E) \equiv \sum_k \int_E^\infty \sigma_{nk}^{r,iso}(E, E') \phi_k^{sa}(x, E') dE', \quad (29)$$

The isotropic component of the charged particles is obtained by solving

$$B[\phi_j^{iso}] = \sum_k \int_E^\infty \sigma_{jk}(E, E') \phi_k^{iso}(x, E') dE', \quad (30)$$

which will be handled later. For the moment, the summations in equation (28)-(30) are taken over all transported particles; the summations will be simplified later based on physical arguments.

We now return to equation (28) and note that the contribution to the secondary neutron field from isotropic, low energy, charged target fragments will be small since the range of these charged particles is small compared to their mean free path length [Wilson et al. 1991] as seen in Fig. 4. Thus, only the neutron projectile – neutron fragment integral need be retained. In this case, the isotropic neutron transport equation reduces to

$$B[\phi_n^{iso}] = \int_E^\infty \sigma_{nn}(E, E') \phi_n^{iso}(x, E') dE' + \eta_n(x, E). \quad (31)$$

The isotropic neutron fluence is now decomposed into forward and backward components according to

$$\phi_n^{iso}(x, E) = \phi_n^f(x, E) + \phi_n^b(x, E). \quad (32)$$

The terms forward and backward have different meanings when applied to fluences and cross sections. The forward component of the isotropic neutron fluence refers to all neutrons propagating in the forward direction; the backward component of the isotropic neutron fluence refers to all neutrons propagating in the backward direction. The forward component of the neutron production cross section refers to those neutrons produced with scattering angle in the interval  $[0, \pi/2]$  (no change in direction of propagation); the backward component of the neutron production cross section refers to those neutrons produced with scattering angle in the interval  $(\pi/2, \pi]$  (change in direction of propagation from forward to backward or vice versa).

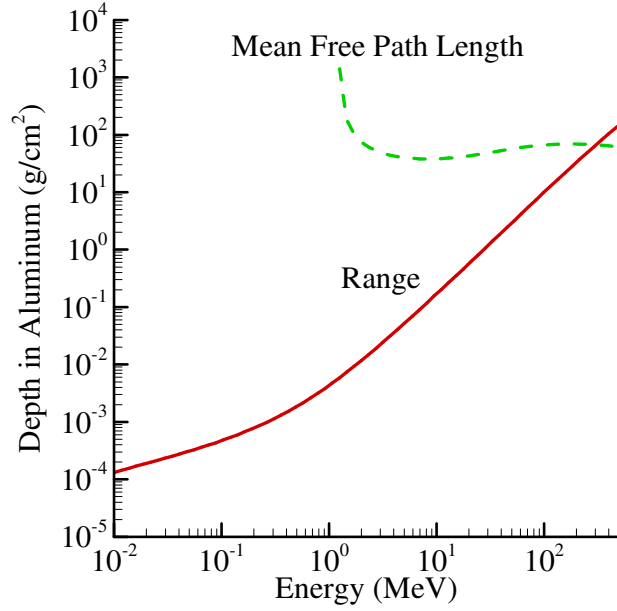


Figure 4. Range and mean free path length of  $^4\text{He}$  in Aluminum.

The nuclear reactive neutron production cross section is assumed to take the form of equation (20), thereby splitting it into forward and backward components. The elastic portion is also decomposed, but it is accomplished by considering the approximate relationship between scattering angle, pre-collision energy ( $E'$ ) and post-collision energy ( $E$ ) given by Haffner [1967]

$$E = E' \left[ \frac{A_T^2 + 2A_T \cos \theta + 1}{(A_T + 1)^2} \right]. \quad (33)$$

Forward scattering occurs for  $\theta \in [0, \pi/2]$  or for  $E' \in [E, E/\beta]$ , and backward scattering occurs for  $\theta \in (\pi/2, \pi]$  or for  $E' \in (E/\beta, E/\alpha]$  where

$$\alpha \equiv \left( \frac{A_T - 1}{A_T + 1} \right)^2, \quad (34)$$

$$\beta \equiv \frac{A_T^2 + 1}{(A_T + 1)^2}. \quad (35)$$

The neutron elastic production cross section is then decomposed into forward and backward components as

$$\sigma_{nn}^{el(+)}(E, E') \equiv \begin{cases} \sigma_{nn}^{el}(E, E'), & E' \in [E, E/\beta] \\ 0, & \text{otherwise} \end{cases}, \quad (36)$$

$$\sigma_{nn}^{el(-)}(E, E') \equiv \begin{cases} \sigma_{nn}^{el}(E, E'), & E' \in (E/\beta, E/\alpha] \\ 0 & , \text{ otherwise} \end{cases} . \quad (37)$$

The complete neutron production cross section can now be expressed as forward and backward components according to

$$\sigma_{nn}(E, E') = \sigma_{nn}^{(+)}(E, E') + \sigma_{nn}^{(-)}(E, E'), \quad (38)$$

with

$$\sigma_{nn}^{(+)}(E, E') \equiv \sigma_{nn}^{el(+)}(E, E') + \sigma_{nn}^{r(+)}(E, E'), \quad (39)$$

$$\sigma_{nn}^{(-)}(E, E') \equiv \sigma_{nn}^{el(-)}(E, E') + \sigma_{nn}^{r(-)}(E, E'). \quad (40)$$

From Feldman [2003], substitution of equations (32) and (38) into equation (31) results in the DC neutron transport model

$$B^{(+)}[\phi_n^f] = \int_E^\infty \sigma_{nn}^{(+)}(E, E') \phi_n^f(x, E') dE' + \int_E^\infty \sigma_{nn}^{(-)}(E, E') \phi_n^b(x, E') dE' + \eta_n^f(x, E), \quad (41)$$

$$B^{(-)}[\phi_n^b] = \int_E^\infty \sigma_{nn}^{(+)}(E, E') \phi_n^b(x, E') dE' + \int_E^\infty \sigma_{nn}^{(-)}(E, E') \phi_n^f(x, E') dE' + \eta_n^b(x, E), \quad (42)$$

with the source terms  $\eta_n^f(x, E)$  and  $\eta_n^b(x, E)$  each taken to be one half of the isotropic source term  $\eta_n(x, E)$ , and the linear differential operators are

$$B^{(+)}[\phi] \equiv \left[ \frac{\partial}{\partial x} + \sigma_n(E) \right] \phi(x, E), \quad (43)$$

$$B^{(-)}[\phi] \equiv \left[ -\frac{\partial}{\partial x} + \sigma_n(E) \right] \phi(x, E). \quad (44)$$

Note that the minus sign in equation (44) accounts for a directional change in propagation. In equation (41), the second integral represents neutrons produced in the forward direction by backward propagating neutrons. In equation (42), the second integral represents neutrons produced in the backward direction by forward propagating neutrons.

Slaba [2007] then showed that by making the simple approximation  $\phi_n^f(x, E) \approx \phi_n^b(x, E)$  one obtains

$$B^{(+)}[\phi_n^f] = \int_E^\infty \sigma_{nn}(E, E') \phi_n^f(x, E') dE' + \eta_n^f(x, E), \quad (45)$$

$$B^{(-)}[\phi_n^b] = \int_E^\infty \sigma_{nn}(E, E') \phi_n^b(x, E') dE' + \eta_n^b(x, E). \quad (46)$$

Equations (45) and (46) define the FB neutron transport model. The physical difference between the models can be deduced by examining the collision integrals. The DC model accounts for multiple changes

of direction (from forward to backward or vice versa) in the coupling source integrals, while the FB model only accounts for a single change of direction. That is, after the initial decomposition of the isotropic neutron source term into forward and backward components, it is assumed in the FB model that all forward neutrons propagate forward, and all backward neutrons propagate backward. The two models will be compared later in the paper.

#### 4. FB Neutron Transport Methods

Heinbockel et al. [2000] and Cloudsley et al. [2000a, 2000b] used a multigroup method for solving the FB neutron transport model. The computational procedure is developed by partitioning the energy grid with respect to the elastic interaction parameter  $\alpha$  defined in equation (34). Equations (45) and (46) are then integrated with respect to energy for some discrete set of energy values. The order of integration is switched in the collision integral and a mean value theorem is applied to evaluate the integrals. The result is an upper triangular system of first order ordinary differential equations solved using back substitution. Though the computational procedure turned out to be relatively efficient, the target dependent energy grid made energy grid convergence testing difficult, and selection of the free parameter in a mean value theorem came down to trial and error for several materials.

Slaba et al. [2006, 2007] and Heinbockel et al. [2007] developed three different methods (collocation method, fixed point series method, and Wilson's method) for solving the FB model and found them to be in good agreement with the multigroup technique. The collocation method [Slaba 2007, Heinbockel et al. 2007] is implemented by assuming that forward and backward neutron fluences can be expressed as a sum of linear basis splines

$$\phi_n^f(x, E) \approx \sum_{j=1}^N B_j(E) \phi_n^f(x, E_j), \quad (47)$$

$$\phi_n^b(x, E) \approx \sum_{j=1}^N B_j(E) \phi_n^b(x, E_j), \quad (48)$$

with

$$B_j(E) \equiv \begin{cases} (E - E_{j-1}) / (E_j - E_{j-1}) & , E \in [E_{j-1}, E_j] \\ (E_{j+1} - E) / (E_{j+1} - E_j) & , E \in (E_j, E_{j+1}] \\ 0 & , \text{ otherwise} \end{cases} \quad (49)$$

The approximations are substituted into the FB model resulting in two upper triangular systems of first order linear ordinary differential equations. Using back substitution, the analytic solution to the systems have been found to be [Slaba 2007, Heinbockel et al. 2007]

$$\begin{aligned} \phi_n^f(x, E_{N-j}) &= e^{a_{N-j, N-j}(x)} \phi_n^f(0, E_{N-j}) + \int_0^x e^{a_{N-j, N-j}(x-x')} \eta_n^f(x', E_{N-j}) dx' \\ &+ (1 - \delta_{j0}) \sum_{k=0}^{j-1} a_{N-j, N-k} \int_0^x e^{a_{N-j, N-j}(x-x')} \phi_n^f(x', E_{N-k}) dx', \end{aligned} \quad (50)$$

$$\begin{aligned} \phi_n^b(x, E_{N-j}) &= e^{a_{N-j, N-j}(L-x)} \phi_n^b(L, E_{N-j}) + \int_x^L e^{a_{N-j, N-j}(x'-x)} \eta_n^b(x', E_{N-j}) dx' \\ &+ (1 - \delta_{j0}) \sum_{k=0}^{j-1} a_{N-j, N-k} \int_x^L e^{a_{N-j, N-j}(x'-x)} \phi_n^b(x', E_{N-k}) dx', \end{aligned} \quad (51)$$

where  $\delta$  is the Kronecker delta,  $L$  is the thickness of the material, and the coefficients  $a_{ij}$  are defined

$$a_{ij} \equiv -\sigma_n(E_i)B_j(E_i) + \int_{E_i}^{\infty} \sigma_{nn}(E_i, E')B_j(E')dE' . \quad (52)$$

The fixed-point series method [Slaba 2007, Heinbockel et al. 2007] is a Neumann series solution to the FB model. The forward and backward components are expressed as

$$\phi_n^f(x, E) = \sum_{k=1}^{\infty} f_0^{(k)}(x, E), \quad (53)$$

$$\phi_n^b(x, E) = \sum_{k=1}^{\infty} b_0^{(k)}(x, E), \quad (54)$$

where the  $k^{th}$  zero order term satisfies the relations

$$B^{(+)}[f_0^{(k)}] = \xi_{k-1}^f(x, E), \quad (55)$$

$$B^{(-)}[b_0^{(k)}] = \xi_{k-1}^b(x, E), \quad (56)$$

and for  $k > 0$ , the  $k^{th}$  set of source terms are defined according to

$$\xi_k^f(x, E) \equiv \int_E^{\infty} \sigma_{nn}(E, E')f_0^{(k)}(x, E')dE', \quad (57)$$

$$\xi_k^b(x, E) \equiv \int_E^{\infty} \sigma_{nn}(E, E')b_0^{(k)}(x, E')dE'. \quad (58)$$

The initial set of source terms  $\xi_0^f(x, E)$  and  $\xi_0^b(x, E)$  are simply the forward and backward components of the isotropic neutron source term  $\eta_n(x, E)$ .

Wilson's method [Slaba et al. 2006, 2007; Heinbockel et al. 2007] is a combination of the collocation method and fixed-point series method. The forward and backward neutron fluences are expressed as the sum of a zero order and first order term by

$$\phi_n^f(x, E) = f_0(x, E) + f_1(x, E), \quad (59)$$

$$\phi_n^b(x, E) = b_0(x, E) + b_1(x, E). \quad (60)$$

Equations (59) and (60) are substituted into the FB model, and it is assumed that the zero order terms satisfy the relations

$$B^{(+)}[f_0] = \eta_n^f(x, E), \quad (61)$$

$$B^{(-)}[b_0] = \eta_n^b(x, E). \quad (62)$$

The FB model is now reduced to

$$B^{(+)}[f_1] = \int_E^\infty \sigma_{nm}(E, E') f_1(x, E') dE' + \xi_1^f(x, E), \quad (63)$$

$$B^{(-)}[b_1] = \int_E^\infty \sigma_{nm}(E, E') b_1(x, E') dE' + \xi_1^b(x, E), \quad (64)$$

where the source terms  $\xi_1^f(x, E)$  and  $\xi_1^b(x, E)$  are calculated from the zero order terms by

$$\xi_1^f(x, E) \equiv \int_E^\infty \sigma_{nm}(E, E') f_0(x, E') dE', \quad (65)$$

$$\xi_1^b(x, E) \equiv \int_E^\infty \sigma_{nm}(E, E') b_0(x, E') dE'. \quad (66)$$

Equations (63) and (64) are solved using the collocation method.

Slaba et al. [2006, 2007] and Heinbockel et al. [2007] showed that the three methods produce almost identical results in a variety of shielding configurations exposed to both SPE and GCR environments and compared well with the multigroup technique in all cases [Slaba 2007]. The work also revealed that the collocation method was the most computationally efficient of the four methods in terms of both memory requirements and run time. Hereafter, any neutron spectra labeled ‘‘FB model’’ are assumed to be generated using the collocation method.

## 5. DC Neutron Transport Methods

Feldman [2003] developed a numerical solution for the DC model. A collocation method was used to discretize the energy spectrum as in equations (47) and (48), and first order finite differencing was used to approximate the spatial derivatives and decouple the transport equations. Discretization of the energy and spatial domains in this way resulted in a large system of linear equations that was solved numerically using LU (Lower-Upper) factorization. LU factorization relies on writing the coefficient matrix as the product of a lower triangular and an upper triangular part so that forward and backward substitution can be used to obtain a solution [Demmel 1997]. It was reported that even single layer slab calculations quickly exhausted the memory capabilities of a desktop PC, and run times of over twenty hours were reported even on specialized computers with adequate memory [Feldman 2003].

We present here a computationally efficient Neumann series solution to the DC model based on the numerical methods verified for the FB model. The forward and backward components of the isotropic neutron fluence are expressed as a sum of zero order terms according to

$$\phi_n^f(x, E) = \sum_{k=1}^{\infty} f_0^{(k)}(x, E), \quad (67)$$

$$\phi_n^b(x, E) = \sum_{k=1}^{\infty} b_0^{(k)}(x, E), \quad (68)$$

where the  $k^{th}$  zero order term satisfies

$$B^{(+)}[f_0^{(k)}] = \int_E^\infty \sigma_{nm}^{(+)}(E, E') f_0^{(k)}(x, E') dE' + \xi_{k-1}^f(x, E), \quad (69)$$

$$B^{(-)}[b_0^{(k)}] = \int_E^\infty \sigma_{nn}^{(+)}(E, E') b_0^{(k)}(x, E') dE' + \xi_{k-1}^b(x, E), \quad (70)$$

and can be solved using the collocation method outlined previously. Note that solutions to equations (69) and (70) include neutron production with scattering angle between 0 and  $\pi/2$ . Neutron production with scattering angle between  $\pi/2$  and  $\pi$  is accounted for in the  $k^{\text{th}}$  set of source terms as

$$\xi_k^f(x, E) \equiv \int_E^\infty \sigma_{nn}^{(-)}(E, E') b_0^{(k)}(x, E') dE', \quad (71)$$

$$\xi_k^b(x, E) \equiv \int_E^\infty \sigma_{nn}^{(-)}(E, E') f_0^{(k)}(x, E') dE', \quad (72)$$

for  $k > 0$ . The initial set of source terms,  $\xi_0^f(x, E)$  and  $\xi_0^b(x, E)$ , are simply the forward and backward components of the isotropic neutron source term  $\eta_n(x, E)$ .

While many terms in the Neumann series are required to adequately resolve the neutron fluence spectra (as many as 75 terms for each component), the computation is quite rapid since the coefficients  $a_{ij}$  used in the collocation method and the cross sections appearing in the source terms in equations (71) and (72) can be pre-calculated and saved for repeated use. No published data exists from Feldman's work, and so any comparisons with data labeled "DC Model" were generated using the proposed Neumann series solution.

## 6. Coupling to Light Ion Transport

In the development of the neutron transport models, we did not solve the isotropic charged particle transport equation

$$B[\phi_j^{iso}] = \sum_k \int_E^\infty \sigma_{jk}(E, E') \phi_k^{iso}(x, E') dE'. \quad (73)$$

At this point, the summation in equation (73) is taken over light particles only. This is justified by noting that  $\phi_j^{iso}$  is associated with low energy target fragments, and heavy ion target fragments are not transported in HZETRN due to their small range [Wilson et al. 1986, 1991, 2006].

The isotropic neutron fluence has already been obtained via one of the bi-directional neutron transport models, and so equation (73) can be expressed in the more explicit form

$$B[\phi_j^{iso}] = \sum_{k \neq n} \int_E^\infty \sigma_{jk}(E, E') \phi_k^{iso}(x, E') dE' + \eta_j(x, E), \quad (74)$$

where the summation is taken over all charged, light particle projectiles ( $k \neq n$ ), and the neutron projectile term has been explicitly written as the source term

$$\eta_j(x, E) \equiv \int_E^\infty \sigma_{jn}(E, E') \phi_n^{iso}(x, E') dE'. \quad (75)$$

We now approximate equation (74) by suppressing the remaining collision integrals. Such an approximation is expected to be valid since the mean free path of these low energy charged particles is

much larger than their range [Wilson et al. 1991] as was seen earlier in Fig. 4. In this case, equation (74) is now reduced to

$$B[\phi_j^{iso}] = \eta_j(x, E), \quad (76)$$

for which an analytic solution exists and is easily found by using the method of characteristics [Haberman 1998]. The solution was given by Wilson et al. [1975] in terms of the nuclear survival probability

$$P_j(E) \equiv \exp \left[ -A_j \int_0^E \frac{\sigma_j(E')}{S_j(E')} dE' \right], \quad (77)$$

and the residual energy  $E_\gamma \equiv R_j^{-1}[x + R_j(E)]$  as

$$\begin{aligned} \phi_j^{iso}(x, E) &= \frac{P_j(E_\gamma) S_j(E_\gamma)}{P_j(E) S_j(E)} \phi_j^{iso}(0, E_\gamma) \\ &+ \int_E^{E_\gamma} \frac{A_j P_j(E')}{P_j(E) S_j(E)} \eta_j[x + R_j(E) - R_j(E'), E'] dE', \end{aligned} \quad (78)$$

where  $R_j(E)$  is given by following the range energy relation

$$R_j(E) = A_j \int_0^E \frac{dE'}{S_j(E')}. \quad (79)$$

Equation (78) can be evaluated rapidly using numerical integration schemes and imposes small memory requirements.

## 7. Results

Solutions to equation (1) using the HZETRN marching algorithm defined by equations (11) and (12) will be labeled “SA” for straight ahead, and it is assumed that all particles (including neutrons) are transported in the forward direction. Solutions to equation (26) using the HZETRN marching algorithm with FB or DC neutrons added and no light ion coupling will be labeled “FB” or “DC”, respectively. Finally, solutions to equation (26) using the HZETRN marching algorithm with FB or DC neutrons and the suggested light ion coupling will be labeled “FBLI” or “DCLI”, respectively. The only difference between FB and FBLI or DC and DCLI is the presence of the light ion coupling term given in the previous section. Therefore, neutron fluences predicted by FB and FBLI (or DC and DCLI) will be identical. In all of the neutron fluence comparisons, FB and DC will be used, but could be interchanged with FBLI and DCLI without consequence.

Results are now given at various depths in a 30 g/cm<sup>2</sup> water target behind a 20 g/cm<sup>2</sup> Aluminum shield exposed to the February 1956 Webber SPE spectrum [Quenby et al. 1959]. The Aluminum shield depth is indicative of spacecraft shielding, and the water depth is indicative of human tissue. This particular SPE spectrum was chosen because of the availability of Monte Carlo data. Fig. 5 shows the forward component of the neutron fluences at 20 g/cm<sup>2</sup> in the water target. The DC model compares quite well to HETC-HEDS and is within the bounds set by FLUKA and MCNPX; the FB and SA solutions predict much higher neutron fluences for energies below 100 MeV. Fig. 6 gives the backward neutron fluences at 20 g/cm<sup>2</sup> in the water target. The DC model again compares well to HETC-HEDS and is within the bounds set by FLUKA and MCNPX; it is a significant improvement over the FB model. There is no backward component of the SA model since all particles are transported in the forward direction. Finally, Fig. 7 gives the total neutron fluence at 20 g/cm<sup>2</sup> in the water target.

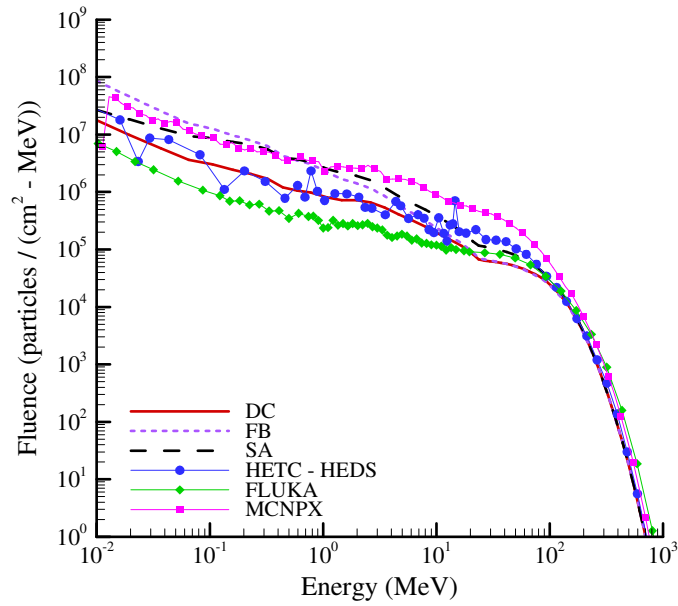


Figure 5. Forward neutron fluence at 20 g/cm<sup>2</sup> in a 30 g/cm<sup>2</sup> water target behind a 20 g/cm<sup>2</sup> Aluminum shield exposed to the February, 1956 Webber SPE.

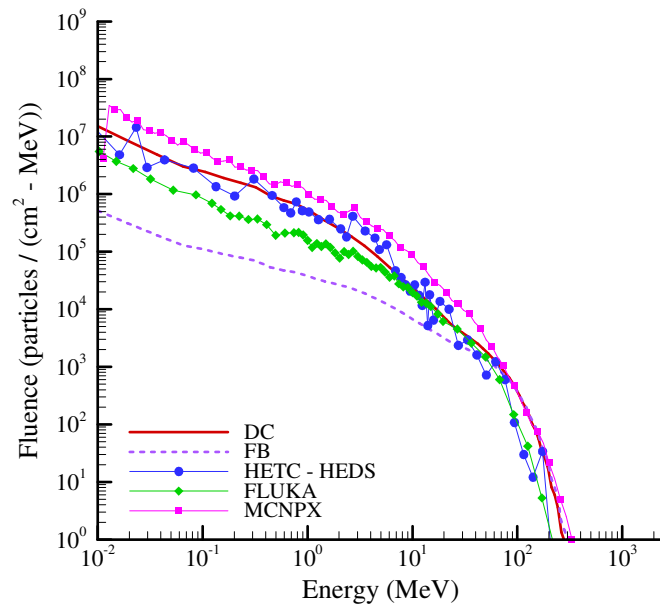


Figure 6. Backward neutron fluence at 20 g/cm<sup>2</sup> in a 30 g/cm<sup>2</sup> water target behind a 20 g/cm<sup>2</sup> Aluminum shield exposed to the February, 1956 Webber SPE.

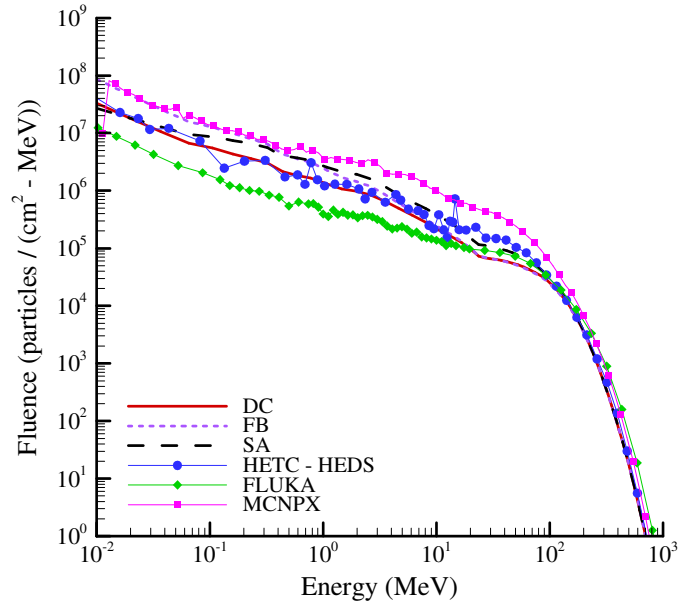


Figure 7. Total neutron fluence at  $20 \text{ g/cm}^2$  in a  $30 \text{ g/cm}^2$  water target behind a  $20 \text{ g/cm}^2$  Aluminum shield exposed to the February, 1956 Webber SPE.

As in each of the previous figures, the DC model compares well to HETC-HEDS and is within the bounds set by FLUKA and MCNPX. Most importantly, it now appears that HZETRN compares as well to the Monte Carlo codes as they compare with each other. Figs. 8-10 give the proton,  $^3\text{H}$ , and  $^4\text{He}$  fluence spectra generated from the SA, FB, DC, FBLI, and DCLI models at  $20 \text{ g/cm}^2$  in the water target. First, note that the spectra predicted by the FB and DC models are identical. This behavior is expected since neither of these models include the suggested light ion coupling, and the charged particle fluences are determined by solutions to equation (26).

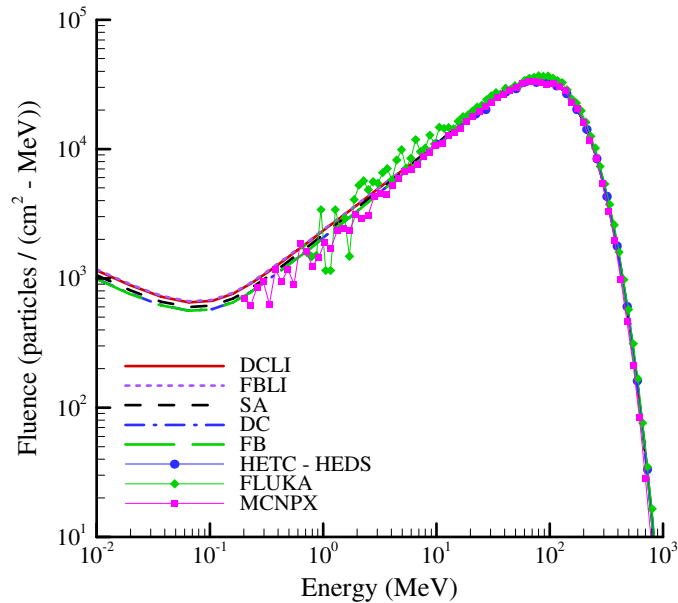


Figure 8. Proton fluence at  $20 \text{ g/cm}^2$  in a  $30 \text{ g/cm}^2$  water target behind a  $20 \text{ g/cm}^2$  Aluminum shield exposed to the February, 1956 Webber SPE.

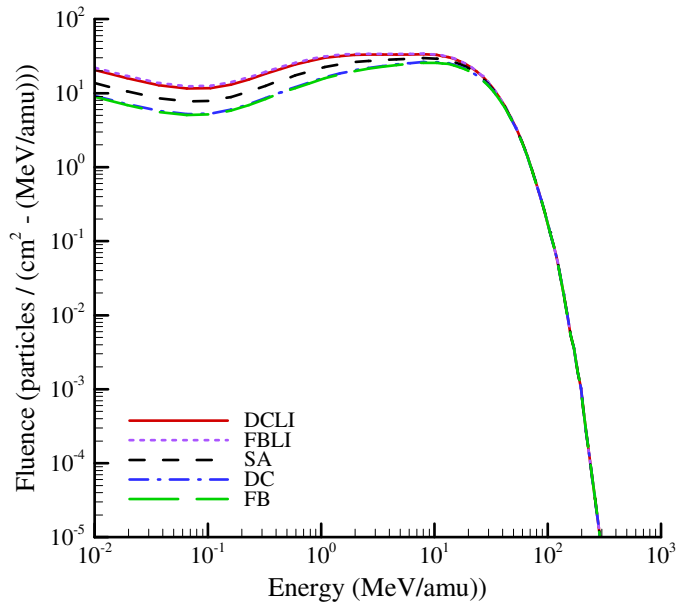


Figure 9.  $^3\text{H}$  fluence at  $20 \text{ g/cm}^2$  in a  $30 \text{ g/cm}^2$  water target behind a  $20 \text{ g/cm}^2$  Aluminum shield exposed to the February, 1956 Webber SPE.

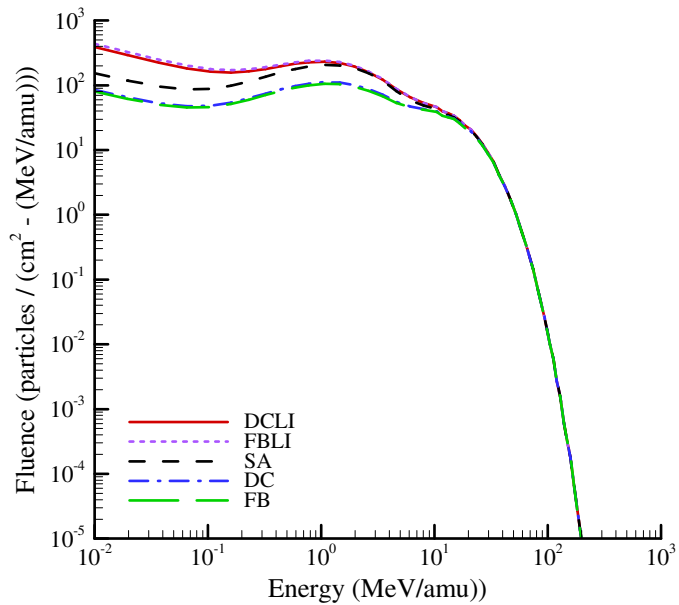


Figure 10.  $^4\text{He}$  fluence at  $20 \text{ g/cm}^2$  in a  $30 \text{ g/cm}^2$  water target behind a  $20 \text{ g/cm}^2$  Aluminum shield exposed to the February, 1956 Webber SPE.

Next, the spectra predicted by the FBLI and DCLI models are similar but not identical. In fact, the FBLI model seems to over-estimate the DCLI model in all three cases. This trend is caused by the light ion coupling source term in equation (74) and the neutron transport model used. If the FB model is used for neutron transport, then the light ion source term in equation (74) will be over predicted and so will the

isotropic light ion fluences. Surprisingly, the FBI and DCLI light ion spectra agree quite well even though the FB and DC neutron fluences in Fig. 7 are almost an order of magnitude different at the lowest energies.

Most importantly, Fig. 9 and Fig. 10 show that a significant reduction in low energy fluence spectra can occur if the suggested light ion coupling term is not included. Though little difference is seen in the proton fluence spectra (Fig. 8), the  $^4\text{He}$  spectrum drops by almost a factor of four if the light ion coupling term is not included. Similar results are also seen for the other light ions transported in HZETRN ( $^2\text{H}$  and  $^3\text{He}$ ). Such deviations can alter integrated quantities as well. For example, Tables 1 and 2 give the dose and dose equivalent values at various depths in the water target. As expected, these values are all reduced if the light ion coupling is not included. Dose and dose equivalent values were not available from FLUKA and MCNPX at the time of this report.

Table 1. Dose (cGy) in a 30 g/cm<sup>2</sup> water target behind 20 g/cm<sup>2</sup> of Aluminum exposed to the February, 1956 Webber SPE spectrum.

Depth g/cm <sup>2</sup>	SA	DCLI	FBLI	DC	FB	HETC- HEDS
0	6.97	6.99	6.98	6.95	6.93	7.20
5	3.78	3.78	3.78	3.75	3.75	4.04
10	2.28	2.28	2.29	2.26	2.26	2.50
20	0.98	0.98	0.99	0.96	0.97	1.10
30	0.49	0.48	0.49	0.47	0.47	0.53

Table 2. Dose equivalent (cSv) in a 30 g/cm<sup>2</sup> water target behind 20 g/cm<sup>2</sup> of Aluminum exposed to the February, 1956 Webber SPE spectrum.

Depth g/cm <sup>2</sup>	SA	DCLI	FBLI	DC	FB	HETC- HEDS
0	11.70	11.83	11.50	11.36	11.03	8.87
5	6.21	6.18	6.27	5.80	5.84	4.85
10	3.94	3.87	4.01	3.56	3.69	3.03
20	1.87	1.79	1.94	1.59	1.71	1.36
30	1.05	0.91	1.07	0.78	0.91	0.63

## 8. Conclusions

A directionally coupled neutron transport model and computationally efficient solution method were presented. Results compared well with HETC-HEDS and were within the bounds set by FLUKA and MCNPX. Therefore, the neutron transport algorithm in HZETRN now agrees with the Monte Carlo codes to the extent that they agree with each other. A first order approximation was also presented for coupling the neutron models to low energy light ion transport, and results indicated that such a coupling is indeed necessary not only for accurate estimates of low energy fluence spectra, but for integrated quantities such as dose and dose equivalent as well. It is recommended that future studies with HZETRN and bi-directional neutrons use the directionally coupled neutron transport model along with the first order light ion coupling presented here.

## 9. Acknowledgments

This research was sponsored by NASA Research Grant NNLO6AA14A. We would like to thank John W. Wilson for his contributions and guidance in this work, Sukesh Aghara for providing the MCNPX data, Larry Townsend, Thomas Handler, and Tony Gabriel for providing the HETC-HEDS data, and Larry Pinsky and Brandon Reddell for providing the FLUKA data.

## 10. References

- Alsmiller, R.G., Irving, D.C., Kinney, W.E., Moran, H.S., The Validity of the Straightahead Approximation in Space Vehicle Shielding Studies, Second Symposium on Protection Against Radiations in Space. NASA Special Publication 71 (1965).
- Briesmeister, J.F. ed., MCNP-A General Monte Carlo N-Particle Transport Code-Version 4C, Los Alamos National Laboratory report LA-13709-M (2000).
- Cloudsley, M.S., Heinbockel, J.H., Kaneko, H., Wilson, J.W., Singleterry, R.C., Shinn, J.L., A Comparison of the Multigroup and Collocation Methods for Solving the Low Energy Neutron Boltzmann Equation. Canadian Journal of Physics, Volume 78, pp. 45-56 (2000a).
- Cloudsley, M.S., Wilson, J.W., Heinbockel, J.H., Tripathi, R.K., Singleterry, R.C., Shinn, J.L., An Improved Elastic and Nonelastic Neutron Transport Algorithm for Space Radiation, NASA Technical Paper 210299 (2000b).
- Cucinotta, F.A., Wilson, J.W., Saganti, P., Hu, X., Kim, M.Y., Cleghorn, T., Zeitlin, C., Tripathi, R.K., Isotopic Dependence of GCR Fluence behind Shielding, Radiation Measurements, Volume 41, pp. 1235-1249 (2006).
- Demmel, J.W., Applied Numerical Linear Algebra, Society for Industrial and Applied Mathematics, Philadelphia (1997).
- Deuflhard, P., Bornemann, F., Scientific Computing with Ordinary Differential Equations, Springer, New York (2002).
- Fasso, A., Ferrari, A., Roesler, S., Sala, P.R., Battistoni, G., Cerutti, F., Gadioli, E., Garzelli, M.V., Ballarini, F., Ottolenghi, A., Empl, A., Ranft, J., The Physics Models of FLUKA: Status and Recent Developments. Computing in High Energy and Nuclear Physics 2003 Conference (CHEP2003), La Jolla, CA, March 24-28, 2003 (paper MOMT005), eConf C0303241 (2003), arXiv:hep-ph/0206267.
- Fasso, A., Ferrari, A., Ranft, J., Sala, P.R., Fluka: A Multi-Particle Transport Code, CERN-2005-10 (2005), INFN/TC\_05/11, SLAC-R-773.
- Feldman, G., A Forward Backward Fluence Model for the Low Energy Neutron Boltzmann Equation, Ph.D. Thesis, Old Dominion University (2003).
- Gabriel, T.A., Bishop, B.L., Alsmiller, F.S., Alsmiller, R.G., Johnson, J.O., Colar95: A Monte Carlo Program Package for the Design and Analysis of Calorimeter systems, ORNL TM-11185 (1995).
- Getselev, I., Rumin, S., Sobolevsky, N., Ufimtsev, M., Podzolkov, M., Absorbed Dose of Secondary Neutrons from Galactic Cosmic Rays Inside the International Space Station, Advances in Space Research, Volume 34, pp. 1429-1432 (2004).
- Haberman, R., Elementary Applied Partial Differential Equations, Prentice Hall, New Jersey (1998).
- Haffner, J.W., Radiation and Shielding in Space, Academic Press, New York (1967).

- Heinbockel, J.H., Cloudsley, M.S., Wilson, J.W., An Improved Neutron Transport Algorithm for Space Radiation. NASA Technical Paper 209865 (2000).
- Heinbockel, J.H., Slaba, T.C., Wilson, J.W., Blattnig, S.R., Cloudsley, M.S., Badavi, F.F., Comparison of Numerical Solution Techniques for Calculating Low Energy Neutrons, SAE ICES 2007 01 3117 (2007).
- Heinbockel, J.H., Slaba, T.C., Blattnig, S.R., Tripathi, R.K., Townsend, L.W., Handler, T., Gabriel, T.A., Pinsky, L.S., Reddell, B., Cloudsley, M.S., Singleterry, R.C., Norbury, J.W., Badavi, F.F., Aghara, S.K., Comparison of the Radiation Transport Codes HZETRN, HETC-HEDS and FLUKA using the February 1956 Webber SPE spectrum, NASA Technical Paper 2009-215560 (2009).
- Marchuk, G.I., Lebedev, V.I., Numerical Methods in the Theory of Neutron Transport, Harwood Academic Publishers, New York (1986).
- MCNPX 2.6.0 Manual, Los Alamos Report LA-CP-07-1473, Los Alamos, April (2008).
- Quenby, J.J. and Webber, W.R., Cosmic Ray Cut-Off Rigidities and the Earth's Magnetic Field, Philosophical Magazine, Volume 4, pp. 90-112 (1959).
- Ranft, J., The FLUKA and KASPRO Hadronic Cascade Codes. Computer Techniques in Radiation Transport and Dosimetry, Plenum Press, pp. 339-371 (1980).
- Shinn, J.L., Wilson, J.W., Lone, M.A., Wong, P.Y., Costen, R.C., Preliminary Estimates of Nucleon Fluxes in a Water Target Exposed to Solar Flare Protons: BRYNTRN Versus Monte Carlo Code, NASA Technical Memo 4565 (1994).
- Slaba, T.C., Heinbockel, J.H., Wilson, J.W., Blattnig, S.R., Cloudsley, M.S., Badavi, F.F., A New Method for Calculating Low Energy Neutron Flux, SAE ICES 2006 01 2149 (2006).
- Slaba, T.C., Three Methods for Solving the Low Energy Neutron Boltzmann Equation, Ph.D. Thesis, Old Dominion University (2007).
- Slaba, T.C., Blattnig, S.R., Cloudsley, M.S., Walker, S.A., Badavi, F.F., An Improved Neutron Transport Algorithm for HZETRN, Advances in Space Research, accepted (2008).
- Townsend, L.W., Miller, T.M., Gabriel, T.A., HETC Radiation Transport Code Development for Cosmic Ray Shielding Applications in Space, Radiation Protection Dosimetry, Volume 115, pp. 135-139 (2005).
- Wilson, J.W., Lamkin, S.L., Perturbation Theory for Charged-Particle Transport in One Dimension. Nuclear Science and Engineering, Volume 57, pp. 292-299 (1975).
- Wilson, J.W., Badavi, F.F., Methods of Galactic Heavy Ion Transport, Radiation Research, Volume 108, pp. 231-237 (1986).
- Wilson, J.W., Townsend, L.W., Schimmerling, W., Khandelwal, G.S., Khan, F., Nealy, J.E., Cucinotta, F.A., Simonsen, L.C., Shinn, J.L., Norbury, J.W., Transport Methods and Interactions for Space Radiations, NASA Reference Publication 1257 (1991).
- Wilson, J.W., Korte, J.J., Sobieski, J., Badavi, F.F., Chokshi, S.M., Martinovic, Z.N., Cerro, J., Qualls, G.D., Radiation Shielding, MDO Processes, and Single Stage to Orbit Design, AIAA Space 2003 Conference, AIAA 2003 6259 (2003).

Wilson, J.W., Tripathi, R.K., Mertens, C.J., Blattnig, S.R., Cloudsley, M.S., Cucinotta, F.A., Tweed, J., Heinbockel, J.H., Walker, S.A., Nealy, J.E., Verification and Validation: High Charge and Energy (HZE) Transport Codes and Future Development, NASA Technical Paper 213784 (2005).

Wilson, J.W., Tripathi, R.K., Badavi, F.F., Cucinotta, F.A., Standardized Radiation Shield Design Method: 2005 HZETRN, SAE ICES 2006 18 (2006).

REPORT DOCUMENTATION PAGE			Form Approved OMB No. 0704-0188		
<p>The public reporting burden for this collection of information is estimated to average 1 hour per response, including the time for reviewing instructions, searching existing data sources, gathering and maintaining the data needed, and completing and reviewing the collection of information. Send comments regarding this burden estimate or any other aspect of this collection of information, including suggestions for reducing this burden, to Department of Defense, Washington Headquarters Services, Directorate for Information Operations and Reports (0704-0188), 1215 Jefferson Davis Highway, Suite 1204, Arlington, VA 22202-4302. Respondents should be aware that notwithstanding any other provision of law, no person shall be subject to any penalty for failing to comply with a collection of information if it does not display a currently valid OMB control number.</p> <p><b>PLEASE DO NOT RETURN YOUR FORM TO THE ABOVE ADDRESS.</b></p>					
1. REPORT DATE (DD-MM-YYYY) 01-10-2009		2. REPORT TYPE Technical Publication		3. DATES COVERED (From - To)	
4. TITLE AND SUBTITLE Coupled Neutron Transport for HZETRN			5a. CONTRACT NUMBER		
			5b. GRANT NUMBER		
			5c. PROGRAM ELEMENT NUMBER		
6. AUTHOR(S) Slaba, Tony C.; Blattnig, Steve R.			5d. PROJECT NUMBER		
			5e. TASK NUMBER		
			5f. WORK UNIT NUMBER 65149.02.07.01		
7. PERFORMING ORGANIZATION NAME(S) AND ADDRESS(ES) NASA Langley Research Center Hampton, VA 23681-2199			8. PERFORMING ORGANIZATION REPORT NUMBER  L-19769		
9. SPONSORING/MONITORING AGENCY NAME(S) AND ADDRESS(ES) National Aeronautics and Space Administration Washington, DC 20546-0001			10. SPONSOR/MONITOR'S ACRONYM(S)  NASA		
			11. SPONSOR/MONITOR'S REPORT NUMBER(S) NASA/TP-2009-215941		
12. DISTRIBUTION/AVAILABILITY STATEMENT Unclassified - Unlimited Subject Category 93 Availability: NASA CASI (443) 757-5802					
13. SUPPLEMENTARY NOTES					
14. ABSTRACT Exposure estimates inside space vehicles, surface habitats, and high altitude aircrafts exposed to space radiation are highly influenced by secondary neutron production. The deterministic transport code HZETRN has been identified as a reliable and efficient tool for such studies, but improvements to the underlying transport models and numerical methods are still necessary. In this paper, the forward-backward (FB) and directionally coupled forward-backward (DC) neutron transport models are derived, numerical methods for the FB model are reviewed, and a computationally efficient numerical solution is presented for the DC model. Both models are compared to the Monte Carlo codes HETC-HEDS, FLUKA, and MCNPX, and the DC model is shown to agree closely with the Monte Carlo results. Finally, it is found in the development of either model that the decoupling of low energy neutrons from the light particle transport procedure adversely affects low energy light ion fluence spectra and exposure quantities. A first order correction is presented to resolve the problem, and it is shown to be both accurate and efficient.					
15. SUBJECT TERMS Space radiation; Transport; Neutron; Light Ion; Dose; Exposure; Shielding					
16. SECURITY CLASSIFICATION OF:			17. LIMITATION OF ABSTRACT	18. NUMBER OF PAGES	19a. NAME OF RESPONSIBLE PERSON
a. REPORT	b. ABSTRACT	c. THIS PAGE			STI Help Desk (email: help@sti.nasa.gov)
U	U	U	UU	31	19b. TELEPHONE NUMBER (Include area code) (443) 757-5802